Inorg. Chem. **2006**, *45*, 7077−7082

Spin-Crossover in an Iron(III)−Bispidine−Alkylperoxide System

Jochen Bautz,[†] Peter Comba,*[,†] and Lawrence Que Jr.*[,‡]

Universität Heidelberg, Anorganisch-Chemisches Institut, Im Neuenheimer Feld 270, D-69120 Heidelberg, Germany, and Department of Chemistry and Center for Metals in Biocatalysis, University of Minnesota, Minneapolis, Minnesota 55455

Received February 13, 2006

The iron(II) complex of a tetradentate bispidine ligand with two tertiary amines and two pyridine groups (L = dimethyl [3,7-dimethyl-9,9′-dihydroxy-2,4-di-(2-pyridyl)-3,7-diazabicyclo nonan-1,5-dicaboxylate]) is oxidized with *tert*-butyl hydroperoxide to the corresponding end-on *tert*-butylperoxo complex $[Fe^{III}(L)(OO^tBu)(X)]^{n+}$ (X = solvent, anion). UV−vis, resonance Raman, and EPR spectroscopy, as a function of the solvent, show that this is a spin-crossover compound. The experimentally observed Raman vibrations for both low-spin and high-spin isomers are in good agreement with those computed by DFT.

Introduction

Mononuclear nonheme iron enzymes play an important role in the metabolism of dioxygen.[1−3] They can activate dioxygen to perform oxidative transformations or convert superoxide to hydrogen peroxide. Iron peroxo or high-valent iron oxo intermediates are considered to be the active species in the catalytic cycles of these enzymes. Examples of biological iron(III) peroxo complexes include those associated with the antitumor drug bleomycin,[4] superoxide reductase,[5−8] and lipoxygenase.[9] For the purple alkylperoxo intermediate of soybean lipoxygenase-3, the crystal structure revealed an end-on alkylperoxo ligand at the iron(III) center.[9] A crystallographic study of the naphthalene dioxygenase−substrate−O_2 complex shows the O_2 to be coordinated in a side-on mode.[10]

In this and other areas of metalloprotein chemistry, low molecular-weight model complexes have been used to thoroughly study the structural and electronic details of the metal sites and to understand the influence of subtle structural changes on the reactivity. In the field of nonheme iron-based dioxygen activation, there has been a great deal of activity in the past decade;[1−3] a number of synthetic iron(III) and iron(IV) intermediates have been thoroughly characterized by spectroscopy,[11−17] and two structures of Fe^{IV}═O complexes have been reported.[15,17] Catalytic activities and corresponding mechanistic proposals have also been discussed in detail.[11,18−20] Many of these studies have been

* To whom correspondence should be addressed. E-mail: peter.comba@aci.uni-heidelberg.de (P.C.); que@chem.umn.edu (L.Q.). Fax: +49-6221-54 66 17 (P.C.).
[†] Universität Heidelberg.
[‡] University of Minnesota.

(1) Costas, M.; Mehn, M. P.; Jensen, M. P.; Que, L., Jr. *Chem. Rev.* **2004**, *104*, 939.
(2) Kovacs, J. *Chem. Rev.* **2004**, *104*, 825.
(3) Kryatov, S. V.; Rybak-Akimova, E. V.; Schindler, S. *Chem. Rev.* **2005**, *105*, 2175.
(4) Burger, R. M. *Chem. Rev.* **1998**, *98*, 1153.
(5) Coulter, E. D.; Emerson, J. P.; Kurtz, D. M., Jr.; Cabelli, D. E. *J. Am. Chem. Soc.* **2000**, *122*, 11555.
(6) Emerson, J. P.; Coulter, E. D.; Cabelli, D. E.; Phillips, R. S.; Kurtz, D. M., Jr. *Biochemistry* **2002**, *41*, 4348.
(7) Maté, C.; Mattioli, T. A.; Horner, O.; Lombard, M.; Latour, J.-M.; Fontecave, M.; Nivière, V. *J. Am. Chem. Soc.* **2002**, *124*, 4966.
(8) Nivière, V.; Asso, M.; Weill, C. O.; Lombard, M.; Guigliarelli, B.; Favaudon, V.; Houée-Levin, C. *Biochemistry* **2004**, *43*, 808.
(9) Skrzypczak-Jankun, E.; Bross, R. A.; Caroll, R. T.; Dunham, W. R.; Funk, M. O., Jr. *J. Am. Chem. Soc.* **2001**, *123*, 10814.
(10) Karlsson, A.; Parales, J. V.; Parales, R. E.; Gibson, D. T.; Eklund, H.; Ramaswamy, S. *Science* **2003**, *299*, 1039.
(11) Girerd, J.-J.; Banse, F.; Simaan, A. J. *Struct. Bonding* **2000**, *97*, 145.
(12) Lehnert, N.; Neese, F.; Ho, R. Y. N.; Que, L., Jr.; Solomon, E. I. *J. Am. Chem. Soc.* **2002**, *124*, 10810.
(13) Roelfes, G.; Vrajmasu, V.; Chen, K.; Ho, R. Y. N.; Rohde, J.; Zondervan, C.; la Crois, R. M.; Schudde, E. P.; Lutz, M.; Spek, A. L.; Hage, R.; Feringa, B.; Munck, E.; Que, L., Jr. *Inorg. Chem.* **2003**, *42*, 2639.
(14) Grapperhaus, C. A.; Mienert, B.; Bill, E.; Weyhermüller, T.; Wieghardt, K. *Inorg. Chem.* **2000**, *39*, 5306.
(15) Rohde, J.-U.; In, J.-H.; Lim, M. H.; Brennessel, W. W.; Bukowski, M. R.; Stubna, A.; Münck, E.; Nam, W.; Que, L., Jr. *Science* **2003**, *299*, 1037.
(16) Lim, M. H.; Rohde, J.-U.; Stubna, A.; Bukowski, M. R.; Costas, M.; Ho, R. Y. N.; Münck, E.; Nam, W.; Que, L., Jr. *Proc. Natl. Acad. Sci., U.S.A.* **2003**, *100*, 3665.
(17) Klinker, E. J.; Kaizer, J.; Brennessel, W. W.; Woodrum, N. L.; Cramer, C., J.; Que, L., Jr. *Angew. Chem. Int. Ed.* **2005**, *44*, 3690.
(18) Klopstra, M.; Roelfes, G.; Hage, R.; Kellogg, R. M.; Feringa, B. L. *Eur. J. Inorg. Chem.* **2004**, 846.
(19) Chen, K.; Costas, M.; Kim, J.; Tipton, A. K.; Que, L., Jr. *J. Am. Chem. Soc.* **2002**, *124*, 3026.
(20) Chen, K.; Costas, M.; Que, L., Jr. *J. Chem. Soc., Dalton Trans.* **2002**, 672.

10.1021/ic0602401 CCC: $33.50
Published on Web 08/03/2006

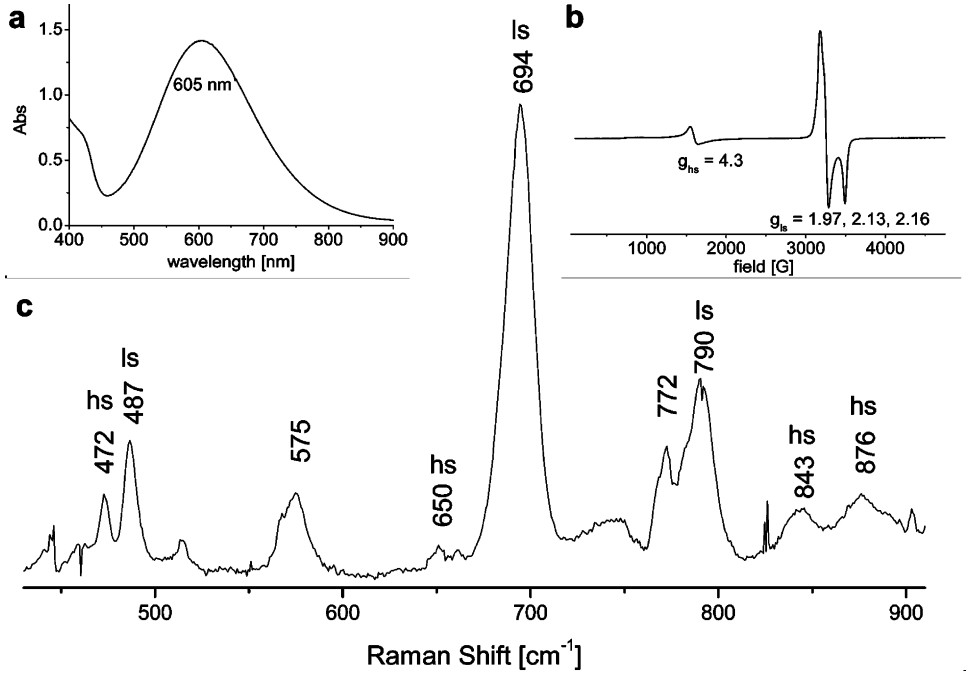

Figure 1. Experimental spectra of 1 mM $[Fe^{III}(L)(OO^tBu)(NCMe)]^{2+}$ in MeCN: (a) electronic (−40 °C), (b) X-band EPR (4 K), and (c) resonance Raman (77 K).

Chart 1

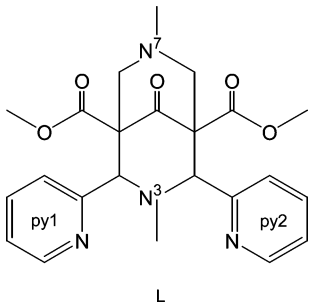

L

based on tetra- and pentadentate derivatives of tpa (tpa = tris-[(2-pyridyl)methyl]amine).

Bispidine-type ligands (see Chart 1 for the tetradentate bispidine ligand L used in this communication; pentadentate bispidine ligands have an additional donor substituted at N3 or N7) provide a useful ligand framework to address questions of relevance to coordination chemistry and bioinorganic chemistry. Of particular importance is the rigidity of these ligands and the easily tunable ligand field and redox properties through variation of the donor set. In general, these ligands produce intermediate ligand fields and, therefore, complexes close to the spin-crossover limit for the various iron oxidation states.[21] Pentadentate bispidine ligands have been found to form relatively stable and well-characterized iron(III) peroxo complexes,[22] which result in interesting reactivities.[23] On the other hand, related chemistry with

Chart 2

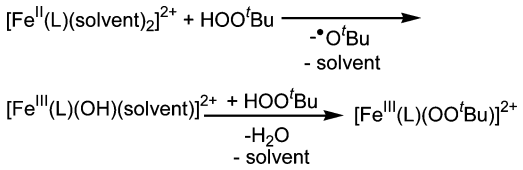

tetradentate bispidine ligands has not yet been reported (i.e., no iron(III) and iron(IV) complexes have been characterized spectroscopically). It was therefore of interest to study the alkylperoxoiron(III) chemistry with bispidine complexes, specifically, because the properties of alkylperoxoiron(III) complexes have been shown to strongly depend on the spin state.[24−26] In this paper, we report spectroscopic and computational studies related to $[Fe(L)(OO^tBu)(X)]^{2+}$ complexes (see Chart 2).

Results and Discussion

Preparation, Spectroscopy, and Reactivity. Treatment of $[Fe^{II}(L)(X)_2]^{2+}$ (X = solvent, anion) with 2 equiv of ^{t}BuOOH at −40 °C in acetonitrile yields, within 15 min, a transient blue intermediate that has an electronic transition at λ_{max} = 605 nm ($\epsilon \approx 1200$ M^{-1} cm^{-1}; Figure 1a). In the EPR spectrum, there are strong signals (MeCN, 4 K) at g = 1.97, 2.13, and 2.16, typical for a low-spin iron(III) complex, and there is a low-intensity signal at g = 4.3, assigned to a high-spin iron(III) complex (Figure 1b). The resonance Raman spectrum of this solution has transitions at 487, 694, and 790 cm^{-1} (Figure 1c). These are almost identical in energy to those observed for the alkylperoxo intermediate

(21) Börzel, H.; Comba, P.; Hagen, K. S.; Merz, M.; Lampeka, Y. D.; Lienke, A.; Linti, G.; Pritzkow, H.; Tsymbal, L. V. *Inorg. Chim. Acta* **2002**, *337*, 407.
(22) Bukowski, M. R.; Comba, P.; Limberg, C.; Merz, M.; Que, L. Jr.; Wistuba, T. *Angew. Chem., Int. Ed.* **2004**, *43*, 1283.
(23) Bukowski, M. R.; Comba, P.; Lienke, A.; Limberg, C.; Lopéz de Laorden, C.; Mas-Ballesté, R.; Merz, M.; Que, L., Jr. *Angew. Chem., Int. Ed.* **2006**, *45*, 3446.
(24) Lehnert, N.; Ho, R. Y. N.; Que, L., Jr.; Solomon, E. T. *J. Am. Chem. Soc.* **2001**, *123*, 8271.
(25) Lehnert, N.; Ho, R. Y. N.; Que, L., Jr.; Solomon, E. I. *J. Am. Chem. Soc.* **2001**, *123*, 12802.
(26) Lehnert, N.; Fujisawa, K.; Solomon, E. I. *Inorg. Chem.* **2003**, *42*, 469.

Table 1. Observed Resonance Raman Transitions of Iron(III) Alkylperoxides

	$\delta_{t-butyl}$ (cm^{-1})	ν_{FeO} (cm^{-1})	ν_{OO} (cm^{-1})	spin state
$[Fe(tpa)(OO^tBu)]^{2+}$ [a]	490	696	796	1/2
$[Fe(6\text{-}Me_3\text{-}tpa)(OO^tBu)]^{2+}$ [b]	468	647	843/881	5/2
$[Fe(L)(OO^tBu)]^{2+}$ (MeCN, 77K)	487	694	790	1/2
$[Fe(L)(OO^tBu)]^{2+}$ (CH_2Cl_2, 77K)	470	652	845/875	5/2

[a] Data from ref 24. [b] Data from ref 25.

derived from $[Fe^{II}(tpa)]^{2+}$ and ^{t}BuOOH (490, 696, and 796 cm^{-1}),[24] suggesting a very similar binding mode.

A normal coordinate analysis was performed for the tpa-based system.[24] Because of the structural similarity of tpa and L (tetradentate amine/pyridine donor ligands with two free positions for substrate binding in the cis configuration) and the closely related spectrum, the same assignments for the Raman transitions were used (see Table 1). Also observed in the resonance Raman spectrum is another set of signals (470, 652, 845, and 875 cm^{-1}; see Figure 1c) that corresponds to known high-spin iron(III) alkylperoxides, such as those of $[Fe^{III}(6\text{-}Me_3\text{-}tpa))(OO^tBu)]^{2+}$ (468, 647, 843, and 881 cm^{-1}) and $[Fe^{III}(Bpz_3)(OO^tBu)]^{2+}$ (Bpz_3 = hydrotris(3-*tert*-butyl-5-isopropyl-1-pyrazolyl)borate).[25] These observations suggest that $[Fe^{III}(L)(OO^tBu)]^{2+}$ in CH_3CN is a mixture of a low-spin and a high-spin iron(III) isomer, similar to what has been observed for $[Fe^{III}(6\text{-Me-tpa}))(OO^tBu)]^{2+}$.[27]

With a system at the spin-crossover limit, one expects significant spectral changes as a function of the solvent. Therefore, the coordinating acetonitrile solvent was substituted by the noncoordinating dichloromethane. Here, it is not evident if the water or hydroxide formed during the reaction is coordinated as the sixth donor or if a pentacoordinated species results. However, in any case, a lower ligand field and, therefore, a larger fraction of the high spin species are expected. These expectations are fulfilled, as shown in Figure 2, where the electronic, resonance Raman, and EPR spectra in the two solvents are shown for comparison: in acetonitrile, the low-spin species with λ_{max} = 605 nm, resonance Raman bands at 487, 694, and 790 cm^{-1}, and EPR g values of 1.97, 2.13, and 2.16 is stabilized, while in dichloromethane, there is preference for the high-spin electronic configuration with λ_{max} = 560 nm, resonance Raman peaks at 470, 652, 845, and 875 cm^{-1}, and EPR g values of 9.4, 7.9, 5.6, and 4.3. [Note that the effect demonstrated here experimentally is a solvent-dependent spin-state switch rather than a spin equilibrium, which classically is demonstrated by variable-temperature measurements. The EPR signals at g ≈ 4 and 2 have been shown by saturation experiments to be from independent species, and the temperature-dependent variation of their intensities has been observed (see Supporting Information). On the basis of the computational data, we assume that the temperature dependence is not exclusively caused by relaxation effects, and therefore, we interpret these data as support for a spin equilibrium.]

The main differences between the high- and low-spin alkylperoxo intermediates are the Fe−O and O−O bond strengths.[24−26] In the high-spin case, one generally observes a weaker Fe−O bond, and in the low-spin species, there

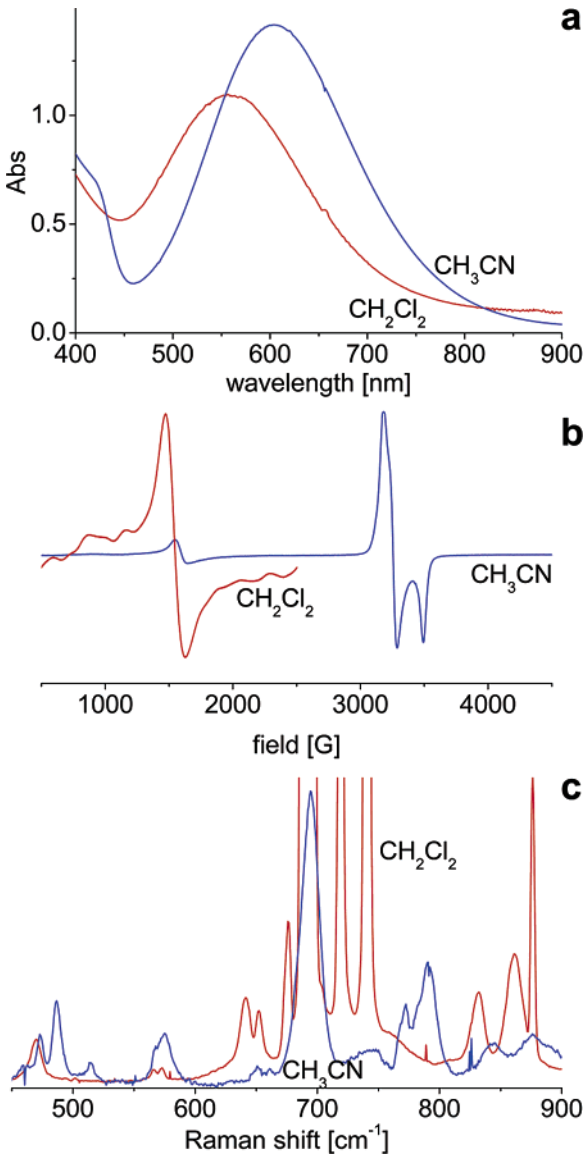

Figure 2. Comparison of the low-temperature experimental spectra of $[Fe(L)(OO^tBu)(X)]^{2+}$ in MeCN and CH_2Cl_2: (a) electronic (−40 °C), (b) X-band EPR (4 K), and (c) resonance Raman (77 K).

usually is an activated O−O bond (see Table 1 for typical resonance Raman data). These differences result in different decay pathways of the meta-stable iron(III) intermediates, with the high-spin species undergoing Fe−OOR bond cleavage[25] and the low-spin complex decaying via a homolytic cleavage of the FeO−OR bond to form Fe^{IV}=O and an alkoxy radical.[25,28,29]

In the tpa-based systems, the reactivity of the Fe^{III}−OOR complex has been shown to be enhanced by the addition of a Lewis base such as pyridine or pyridine-*N*-oxide.[28] The influence of pyridine-*N*-oxide on the reactivity of $[Fe^{III}(L)(OO^tBu)(X)]^{2+}$ was thus tested in acetonitrile and dichloromethane. As expected and in agreement with the

(27) Zang, Y.; Kim, J.; Dong, Y.; Wilkinson, E. C.; Appelman, E. H.; Que, L., Jr. *J. Am. Chem. Soc.* **1997**, *119*, 4197.
(28) Kaizer, J.; Costas, M.; Que, L., Jr. *Angew. Chem., Int. Ed.* **2003**, *42*, 3671.
(29) Mairata i Payeras, A.; Ho, R. Y. N.; Fujita, M.; Que, L., Jr. *Chem.—Eur. J.* **2004**, *10*, 4944.

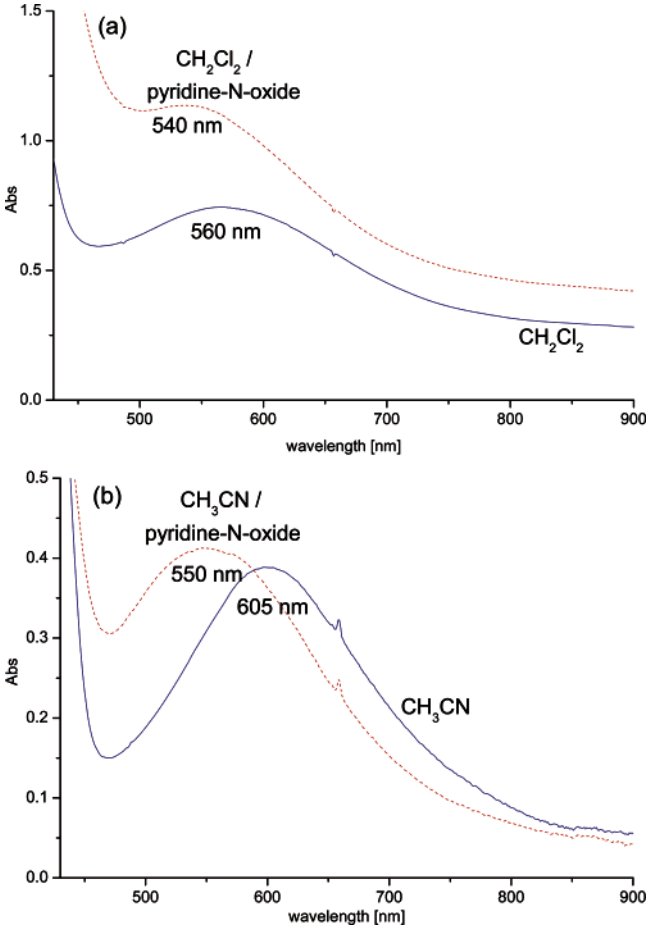

Figure 3. Addition of pyridine-*N*-oxide to $[Fe^{III}(L)(OO^tBu)(X)]^{2+}$ at −40 °C in (a) CH_2Cl_2 and (b) MeCN.

observations with similar systems,[30] in CH_2Cl_2, a 20 nm shift of the maximum in the electronic absorption to 540 nm was observed (see Figure 3a). Interestingly, a similar blue shift of the maximum from 605 to 550 nm in MeCN was observed after the addition of pyridine-*N*-oxide (see Figure 3b), in contrast to the tpa-based chemistry, where the addition of the Lewis base accelerated the decay to a high-valent ferryl species.[28] The EPR spectrum of a solution of $[Fe^{III}(L)(OO^tBu)(X)]^{2+}$ in CH_3CN shows, after the addition of pyridine-*N*-oxide, a typical spectrum for high-spin iron(III), with signals at $g = 8.8$, 6.5, and 4.3, in agreement with the observations in the electronic spectra. This change may be caused by the fast reaction of the Lewis base with the high-spin species in equilibrium with the major low-spin component. Alternatively, the observation is also consistent with the displacement of the MeCN ligand with pyO in the low-spin complex, which then converts the metal center to high spin.

Computational Analysis. There are two isomers of $[Fe^{III}(L)(OO^tBu)(X)]^{2+}$ (X = solvent), with either the alkylperoxide or the solvent in-plane with the two trans-disposed pyridine rings (see Figure 4). A general observation with the bispidine ligands is that coordination trans to N3 (in-plane with the two pyridine donors) is stronger than that

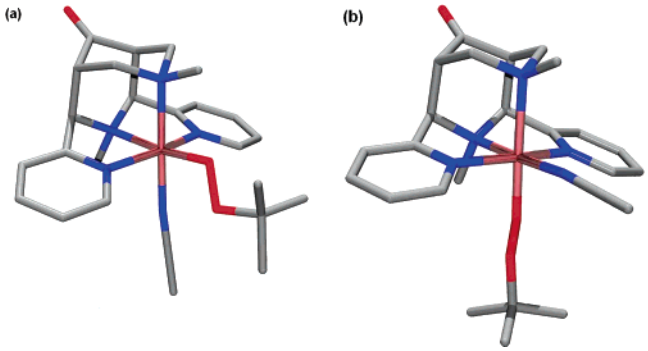

Figure 4. DFT structures of $[FeL(OO^tBu)(CNMe)]^{2+}$, ls, isomers a and b.

trans to N7.[22,23,31,32] This is probably because the pyridine groups are weak π acceptors, and the in-plane coordination of π donors (such as $^tBuOO^-$, Cl^- etc.) may lead to an enhancement of their binding in-plane with the pyridine donors. DFT calculations were carried out to optimize the structures of the two isomers of $[Fe^{III}(L)(OO^tBu)(X)]^{2+}$ with various coligands (X = OH_2, OH^-, $NCCH_3$, as well as the five-coordinate complex), all in high- and low-spin electronic configurations, together with the corresponding tpa and 6-Me_3-tpa complexes (also including the two possible isomers and spin states). Some structural data are listed in Table 2, and the computed Raman transitions (together with the experimental data for comparison) are presented in Table 3.

The calculated structural data (Table 2) indicate that the $Fe^{III}-OO^tBu$ bond is significantly longer in the high-spin than in the low-spin configuration, in agreement with the expected differences resulting from the different electronic ground state and the observed Raman frequencies discussed above. Within a given spin state, these bonds are nearly constant over the entire series of computed structures. Also, as expected, the $Fe^{III}O-O^tBu$ distances are longer in the low-spin than in the high-spin configuration, and again, these bond distances are fairly constant over the entire series of structures. The differences in the series of structures are somewhat larger in the high-spin state than in the low-spin configuration, and there seems to be a correlation with the π-bonding properties of the coligands, consistent with the π-bonding interpretation given above. There is acceptable agreement between observed and computed Raman bands (see Table 3), and this supports the present and published assignments[24−26] (see Table 1). However, the differences between the vibrational frequencies in the two sets of isomers and with the various coligands are too small to allow a meaningful characterization.

The computed differences in total energies between the low- and high-spin forms are listed in Table 4. For the tpa-based systems, these are in agreement with the experiments (i.e., with the unsubstituted ligand the iron(III) alkylperoxo complexes are predicted to be low spin, while those with the methyl-substituted ligand are predicted to be high spin,

(30) Bukowski, M. R.; Halfen, H. L.; van den Berg, T. A.; Halfen, J. A.; Que, L., Jr. *Angew. Chem.* **2005**, *117*, 590.
(31) Comba, P.; Kerscher, M.; Roodt, A. *Eur. J. Inorg. Chem.* **2004**, *23*, 4640.
(32) Comba, P.; Lienke, A. *Inorg. Chem.* **2001**, *40*, 5206.

Table 2. Calculated Structural Parameters of Iron(III) Alkylperoxides (Gaussian 03, B3LYP, 6-31G*)

isomer a

		FeL/OO^{t}Bu/MeCN	FeL/OO^{t}Bu/H_2O	FeL/OO^{t}Bu/OH	FeL/OO^{t}Bu/MeCN (5-coordinate)	Fetpa/OO^{t}Bu/MeCN[a]
r(FeO) (Å)	ls	1.78	1.79	1.80	1.74	1.78
	hs	1.91	1.88	1.89	1.89	1.86
r(OO) (Å)	ls	1.42	1.45	1.46	1.42	1.43
	hs	1.38	1.41	1.44	1.40	1.40

isomer b

		FeL/OO^{t}Bu/MeCN	FeL/OO^{t}Bu/H_2O	FeL/OO^{t}Bu/OH	FeL/OO^{t}Bu/MeCN (5-coordinate)	Fetpa/OO^{t}Bu/MeCN[b]
r(FeO) (Å)	ls	1.78	1.79	1.81		1.79
	hs	1.86	1.86	1.87		1.92
r(OO) (Å) ls	ls	1.43	1.46	1.46		1.42
	hs	1.40	1.42	1.45		1.38

[a] Solvent trans to amine. [b] Solvent trans to pyridine.

Table 3. Calculated Vibrations of the Alkylperoxides (Gaussian 03, B3LYP, 6-31G*)

low-spin alkylperoxides (isomer a/b)

	FeL/OO^{t}Bu/exp	FeL/OO^{t}Bu/MeCN	FeL/OO^{t}Bu/H_2O	FeL/OO^{t}Bu/OH	FeL/OO^{t}Bu (5-coordinate)	Fe(tpa)/OO^{t}Bu/MeCN (exptl)[a]
ν(FeO) (cm^{-1})	694	700/703	678/686	677/666	710	709/700 (696)
ν(OOC) (cm^{-1})	*b*	842/842	823/855	877/873	822	847/846
ν(OO) (cm^{-1})	790	869/860	867/858	903/897	908	867/870 (796)

High spin alkylperoxides (isomer a/b)

	FeL/OO^{t}Bu/exp	FeL/OO^{t}Bu/MeCN	FeL/OO^{t}Bu/H_2O	FeL/OO^{t}Bu/OH	FeL/OO^{t}Bu (5-coordinate)	Fe(6-Me_3-tpa)/OO^{t}Bu/MeCN (exptl)[a]
ν(FeO) (cm^{-1})	652	599/622	606/630	641/659	628	614/593 (637)
ν(OOC) (cm^{-1})	845	811/816	809/812	861/860	800	818/812 (842)
ν(OO) (cm^{-1})	875	930/902	895/894	914/910	889	890/931 (876)

[a] Experimental data from refs 24 and 25. [b] Not resolved.

Table 4. Calculated Energy Differences between the High- and Low-Spin Forms of the Iron(III) Alkylperoxides (Gaussian 03, B3LYP/6-31G*), Corrected for Zero-Point Energies

	ΔE(ls−hs) (kJ/mol)
$[Fe(L)(OO^tBu)(NCMe)]^{2+}$ [a]	11.0
$[Fe(L)(OO^tBu)(NCMe]^{2+}$ [b]	12.5
$[Fe(L)(OO^tBu)(H_2O)]^{2+}$ [a]	16.1
$[Fe(L)(OO^tBu)(H_2O)]^{2+}$ [b]	19.6
$[Fe(L)(OO^tBu)(OH)]^{+}$ [a]	43.9
$[Fe(L)(OO^tBu)(OH)]^{+}$ [b]	45.3
$[Fe(L)(OO^tBu)]^{2+}$ (5-coord) [a]	37.4
$[Fe(tpa)(OO^tBu)(NCMe)]^{2+}$ [a]	−4.8
$[Fe(tpa)(OO^tBu)(NCMe)]^{2+}$ [b]	−10.0
$[Fe(6\text{-}Me_3\text{-}tpa)(OO^tBu)(NCMe)]^{2+}$ [a]	41.0
$[Fe(6\text{-}Me_3\text{-}tpa)(OO^tBu)(NCMe)]^{2+}$ [b]	31.4

[a] Isomer a with the solvent trans to N^3 (trans to the amine of tpa). [b] Isomer b with the solvent trans to N^7 (trans to a pyridine of tpa).

as observed experimentally).[25] Also, the $[Fe^{III}(L)(OO^tBu)(X)]^{n+}$ complexes (both isomers) with X = OH_2, OH^- or as a five-coordinate complex are predicted to be high spin. However, with NCMe as a coligand, the energy difference is only around 10 kJ mol^{-1}, consistent with the observation of a high-/low-spin mixture in this solvent. Within the expected error limit of DFT energies with the methods used (e.g., solvation neglected), the observed trends support the experimental observations and the computed data may be considered to be in agreement with the experiment.

Conclusion

The $[Fe^{III}(L)(OO^tBu)(X)]^{2+}$ complex is shown to be a spin-crossover system. The equilibrium between the high- and low-spin states can be influenced by the solvent (X = MeCN, CH_2Cl_2, 77 K), and the high- and low-spin forms may be specifically stabilized. This is in agreement with DFT calculations, which have also been used to fully assign the relevant resonance Raman transitions.

Experimental Section

Measurements and Materials. All commercially available reagents were used as purchased. The bispidine ligand, L, was prepared according to standard literature procedures.[33] The EPR spectra were recorded on a Bruker EPP 300 spectrometer equipped with an Oxford ESR910 liquid helium cryostat and an Oxford temperature controller or on a Bruker ELEXSYS E500 system using a liquid nitrogen cryostat. Resonance Raman spectra were collected on an Acton AM-506 spectrometer (1200-goove grating) using Kaiser optical holographic super-notch filters with a Princeton Instruments liquid N_2-cooled (LN-1100PB) CCD detector with a 4 or 2 cm^{-1} spectral resolution. Spectra were obtained by a back-scattering geometry on liquid N_2-frozen samples using a Spectra Physics argon/krypton laser. UV−vis spectra were recorded on an HP 8453A diode array spectrometer. Low-temperature visible spectra were obtained using a USP-203 cryostat from UNISOKU Scientific Instruments, Japan, and on a J&M Tidas II.

Preparation of $[Fe(L\cdot H_2O)(OH_2)_2](BF_4)_2$. A solution 3.0 g of ligand L in 30 mL of dry acetonitrile was added to a solution of 2.3 g of $Fe(BF_4)_2\cdot 6\,H_2O$ in 30 mL of acetonitrile, and the mixture was stirred for 4 h. The solvent was reduced to 5 mL under vacuum, and a yellow solid was precipitated with Et_2O, which was recrystallized from MeCN/Et_2O under an inert atmosphere. Anal. Calcd for $C_{23}H_{26}B_2F_8FeN_4O_5\cdot 3H_2O$ (fw 721.98): C, 38.26; H, 4.47;

N, 7.76. Found: C, 37.67; H, 4.55; N, 7.78. UV−vis (MeCN): λ 394 nm ($\epsilon = 1350\ M^{-1}\ cm^{-1}$), 421 ($\epsilon = 1440\ M^{-1}\ cm^{-1}$), 555 nm ($\epsilon = 50\ M^{-1}\ cm^{-1}$)

Formation of the Alkylperoxo Intermediate. Two equivalents of ^{t}BuOOH solution (0.1 mL) was added to a 1 mM solution of $[FeL](BF_4)_2$ in 2 mL of the solvent at −40 °C. MeCN or CH_2Cl_2 was used as solvent. In MeCN, the ^{t}BuOOH solution was prepared from a 70% (7.3 M) ^{t}BuOOH/H_2O solution in MeCN, and in CH_2Cl_2, a 5.5 M ^{t}BuOOH solution in decane was used. The reaction was monitored with UV−vis spectroscopy. Pyridine-*N*-oxide was added, where required, in a 25-fold excess as soon as maximum formation of the Fe^{III}−OOR intermediate was detected (after approximately15 min).

Computational Methods. A simplified model system for the bispidine ligand, in which the ester side chains at C1 and C5 of the ligand backbone are replaced by H atoms (see Chart 1) was used in all calculations. All structures were fully optimized in the gas phase using Gaussian03.[34] For all calculations, the DFT method B3LYP[35] with the standard 6-31G(d)[36] basis set was used. Frequency calculations were performed on all optimized structures to verify their status as true minima on the potential energy surface and to obtain zero-point corrections to the energies. All frequencies were scaled using a factor of 0.9804.

Acknowledgment. Financial support by the German Science Foundation (DFG) and the US National Institutes of Health (GM33162) is gratefully acknowledged.

Supporting Information Available: EPR spectrum of $[Fe(L)(OO^tBu)]^{2+}$. This material is available free of charge via the Internet at http://pubs.acs.org.

IC0602401

(33) Siener, T.; Cambareri, A.; Kuhl, U.; Englberger, W.; Haurand, M.; Koegel, B.; Holzgrabe, U. *J. Med. Chem.* **2000**, *43*, 3746.

(34) Frisch, M. J.; Trucks, G. W.; Schlegel, H. B.; Scuseria, G. E.; Robb, M. A.; Cheeseman, J. R.; Montgomery, J. A., Jr.; Vreven, T.; Kudin, K. N.; Burant, J. C.; Millam, J. M.; Iyengar, S. S.; Tomasi, J.; Barone, V.; Mennucci, B.; Cossi, M.; Scalmani, G.; Rega, N.; Petersson, G. A.; Nakatsuji, H.; Hada, M.; Ehara, M.; Toyota, K.; Fukuda, R.; Hasegawa, J.; Ishida, M.; Nakajima, T.; Honda, Y.; Kitao, O.; Nakai, H.; Klene, M.; Li, X.; Knox, J. E.; Hratchian, H. P.; Cross, J. B.; Adamo, C.; Jaramillo, J.; Gomperts, R.; Stratmann, R. E.; Yazyev, O.; Austin, A. J.; Cammi, R.; Pomelli, C.; Ochterski, J. W.; Ayala, P. Y.; Morokuma, K.; Voth, G. A.; Salvador, P.; Dannenberg, J. J.; Zakrzewski, V. G.; Dapprich, S.; Daniels, A. D.; Strain, M. C.; Farkas, O.; Malick, D. K.; Rabuck, A. D.; Raghavachari, K.; Foresman, J. B.; Ortiz, J. V.; Cui, Q.; Baboul, A. G.; Clifford, S.; Cioslowski, J.; Stefanov, B. B.; Liu, G.; Liashenko, A.; Piskorz, P.; Komaromi, I.; Martin, R. L.; Fox, D. J.; Keith, T.; Al-Laham, M. A.; Peng, C. Y.; Nanayakkara, A.; Challacombe, M.; Gill, P. M. W.; Johnson, B.; Chen, W.; Wong, M. W.; Gonzalez, C.; Pople, J. A. *Gaussian 03*, revision B.03; Gaussian, Inc: Pittsburgh, PA, 2003.

(35) Becke, A. D. J. *J. Chem. Phys. B* **1993**, *98*, 5648.

(36) Hehre, W. J.; Ditchfield, R.; Pople, J. A. *J. Chem. Phys.* **1972**, *56*, 2257.